Wave Equation of Suppressed Traffic Flow Instabilities

Berthold K. P. Horn and Liang Wang

***Abstract*— Traffic congestion wastes fuel and commuters' time, and adds to CO_2 emissions. Stop-and-go traffic instabilities can be suppresses using bilateral control—which differs from "car following" and adaptive cruise control in that, counter-intuitively, it uses information about the *following* vehicle (as well as about the leading vehicle). Stability can be proven mathematically, and can be demonstrated in simulation. A physical analog of a sequence of vehicles using bilateral control is a chain of masses connected by springs and dampers—a system which is inherently stable, since it lacks an external energy source. Here, in order to further understand bilateral control and its capacity to suppress instabilities, we move from a microscopic view (interaction of individual vehicles) to a macroscopic view (densities and flow rates). This leads us to the damped wave equation governing traffic under bilateral control. That equation allows us to determine the speed of propagation of disturbances, as well as their rate of decay. The equation is also useful in fine tuning parameters of bilateral control systems.**

***Index Terms*— Traffic flow instabilities, phantom traffic jam elimination, stop-and-go traffic prevention, car following model, bilateral control, advanced cruise control, adaptive cruise control, damped wave equation.**

I. Background

THE average urban commuter in the USA spends 38 hours per annum stuck in traffic, and as a result wastes 72 liters (19 gallons) of fuel, which adds an extra 172 kgs (380 lbs) of CO_2 to the atmosphere [2]. Overall, in the USA alone, the costs of congestion are estimated to be around $121 billion per annum ($820 per commuter), with 11 billion liters (2.9 billion gallons) of fuel wasted, and 25.4 billion kgs (56 billion lbs) of extra CO_2 emitted [2]. There are also indications that speed variability may be correlated with increased accident incidence [3], [4].

One form of congestion is common stop-and-go traffic flow. It has been shown that bilateral control suppresses traffic flow instabilities [1], [5], [6]. In distinction, it is well known that sequences of car following vehicles—whether controlled by humans or some form of automation such as adaptive cruise control—are subject to instabilities [7]–[25]. (Here "unstable" means amplifying perturbations—see Appendix A and [1]). The formation of a phantom traffic jams is an "emergent property" of a system composed of a coupled chain of cars with drivers.

Manuscript received September 9, 2015; revised January 27, 2016, July 20, 2016, December 14, 2016, May 22, 2017, and August 20, 2017; accepted October 19, 2017. Date of publication December 6, 2017; date of current version September 7, 2018. The Associate Editor for this paper was B. F. Ciuffo. *(Corresponding author: Berthold K. P. Horn.)*

B. K. P. Horn is with the Department of Electrical Engineering and Computer Science, Massachusetts Institute of Technology, Cambridge, MA 02139 USA (e-mail: bkph@csail.mit.edu).

L. Wang is with CSAIL, Massachusetts Institute of Technology, Cambridge, MA 02139 USA (e-mail: wangliang@csail.mit.edu).

Digital Object Identifier 10.1109/TITS.2017.2767595

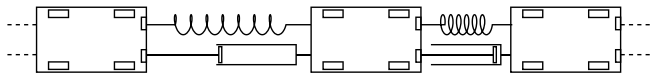

Fig. 1. Mechanical analog of bilateral control. (Note that there can be no such mechanical analog for car following control).

In the car following paradigm, each vehicle adjusts its motion based on the distance to, and the relative speed of the vehicle ahead. In bilateral control, in contrast, the distance to and relative speed of the *following* vehicle is also used. This counter-intuitive additional control input makes the system stable. Roughly speaking, in bilateral control, each vehicle tries to be half way between the leading and the following vehicles (at least, when they have similar speeds, and neither of them is too far away). The suppression of instabilities can be proven using what is essentially a Lyapunov function [1], or using properties of eigenvalues and eigenvectors of matrices [6], and can be demonstrated using simulation.

Vehicles using bilateral control can be modelled as masses connected by springs and dampers (Fig. 1). It is not hard to predict how such a system will respond to perturbations. First, in the absence of damping, waves will propagate in both directions from the point where the perturbation is applied—with speed $v = h\sqrt{k/m}$, where k is the spring constant, m is the mass of the interconnected masses, and h is their separation. The dampers attenuate these waves so that they dissipate with distance and time; the energy of such a coupled physical system decays toward zero. This is in contrast to the amplification of waves that occurs in car following [1]—for which, by the way, there can be no physical model such as that in Fig. 1.

One way to implement bilateral control is to modify "adaptive cruise control" which uses forward facing sensors to implement car following control. Bilateral control can be implemented by the addition of *rear facing* sensors and modification of the control. For an automated system, "looking back" is no harder than "looking forward."

To further study bilateral control and its ability to suppress instabilities, it is of interest to advance from the microscopic view (interactions of individual vehicles) to a macroscopic view (densities and flow rates). We arrive here at the damped wave equation governing a system using bilateral control. This equation can be used to study the propagation and attenuation of disturbances, as well as for fine tuning parameters of the feedback control systems.

The main contribution of this paper is the development of the damped wave equation that governs a line of traffic under

bilateral control. Significantly, this damped wave equation does not have the usual form where horizontal distance along the road is the independent variable. Another contribution is the realization that the "damping" component (a term depending on differences of speeds of adjacent vehicles) is critical to the dissipation of perturbations (that is, making use of distances to neighboring vehicles, for and aft, is *not* sufficient). Finally, we show that symmetric weighting of information from leading and following vehicles is best in that it removes constraints on the relationship between proportional and velocity gains.

Note that this paper is not about explaining where "phantom traffic jams" come from under "traditional" driving conditions. There are literally hundreds of papers on traffic flow instabilities (for a small, but representative sample see [7]–[25]). Our purpose is also *not* to survey papers on traffic flow instabilities (for that see e.g. [26]–[30]), nor is it to make comparisons of various explanations for their origin (cellular automata, fluid flow models, shock waves, eigenvalues of ODEs etc.). This paper is about the bilateral control method for *suppressing* traffic flow instabilities (for an introduction to bilateral control see [1]). The analysis presented here, except for the background description of the car-following model, does not apply to "traditional" traffic, but to traffic under bilateral control.

A reviewer kindly brought to our attention three papers that relate to "bi-directional control," that take into account some information about the following vehicle [31]–[33]. These are related to our work on bilateral control, but do not propose what we do. For one thing, they do not include the all important "damper" term which depends on differences of speeds. This term is important in suppressing travelling waves resulting from perturbations. We also present a physical analog that lends intuitive insight—something that is not possible with their models.

In the case of Nakayama *et al.* [31], "stability" means that the amplitude of oscillation of the leading vehicle will not be amplified as the perturbation is passed from vehicle to vehicle. Because of the non-linearity of their model, they can consider only infinitesimal departures from an equilibrium state. Their non-linear model does not lend itself to the analysis possible with our linear bilateral control rule, and so they are not able to present the kinds of results we do, such as a damped wave equation.

They show that for high enough gain their system can damp out infinitesimal perturbations. However, the gain required may be quite high and lead to accelerations that are uncomfortable for passengers. The authors appear aware of the problem since they emphasize an advantage of their system being that it does not need a gain quite as high as an earlier "optimum velocity" model.

Finally, their model is asymmetrical in that more weight is given to information about the leading vehicle than the following vehicle (in a footnote they explicitly exclude the symmetrically weighed case). In simulation, for example, they use weights of 0.7 and 0.3 for control inputs based on the distances from the leading and following vehicle respectively. We find that giving equal weight to information about leading and following vehicles leads to stability *without* constraints on gains.

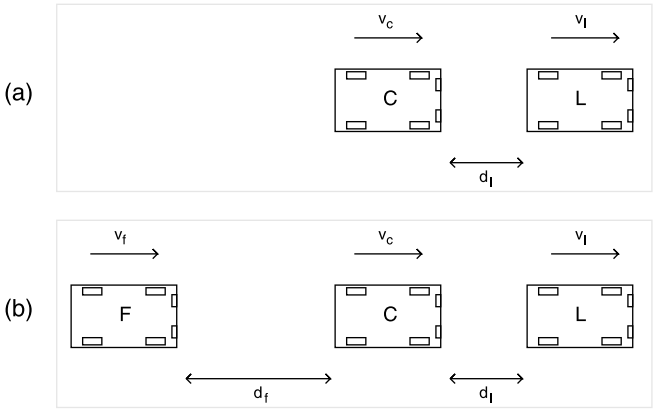

Fig. 2. Vehicles and their relative positions and speeds. (a) In car following, the acceleration of the controlled vehicle 'C' is based only on the relative position and speed of the leading vehicle 'L' (b) In bilateral control, in contrast, the acceleration of vehicle 'C' is based on the relative position and speeds of *both* the following vehicle 'F' and the leading vehicle 'L'.

In the case of Zheng *et al.* [32], it should be noted that they are trying to build a more accurate model of *existing* traffic, not develop a new control rule to suppress traffic flow instabilities. In their context, "bi-directional" means: "If the following car approaches rapidly, then maybe some drivers will choose to change lanes." This is different from an automated system that adjusts the acceleration continuously based on differences in position and speed.

Finally, Treiber and Helbing [33] "bi-directional" system does not introduce the crucial "damper" terms proportional to differences in speed, and so will not have waves of perturbation decaying —in fact, they do not think of their system in terms of propagating waves.

Different from existing bi-directional control methods we show that a simple linear model can suppress traffic flow instabilities effectively. We find that there are three key points to suppressing traffic flow instabilities: (a) use information about the following as well as the leading vehicles; (b) use the relative speeds of the leading and following vehicles (i.e. include "damping" terms), and (c) emphasize the control contributions of leading and following vehicles equally. In order to properly suppress instabilities and dissipate disturbances, we find that it is best to weight contributions equally. This removes constraints on the control system gains and enables use of lower gains than would otherwise be the case.

II. Review of Bilateral Control

Bilateral control can be thought of as a modification of the car-following model. In car following, the acceleration a_c of the controlled vehicle 'C' is dependent on the distance $d_l = (x_l - x_c - l)$ to the leading vehicle 'L' and its relative speed $(v_c - v_l)$ (see Fig. 2(a)) (where l is the length of the vehicle). In bilateral control, in distinction, the acceleration a_c of the controlled vehicle 'C' is dependent on the distance $d_f = (x_c - x_f - l)$ of the following vehicle 'F' and its relative speed, $(v_c - v_f)$ *as well* (see Fig. 2(b)).

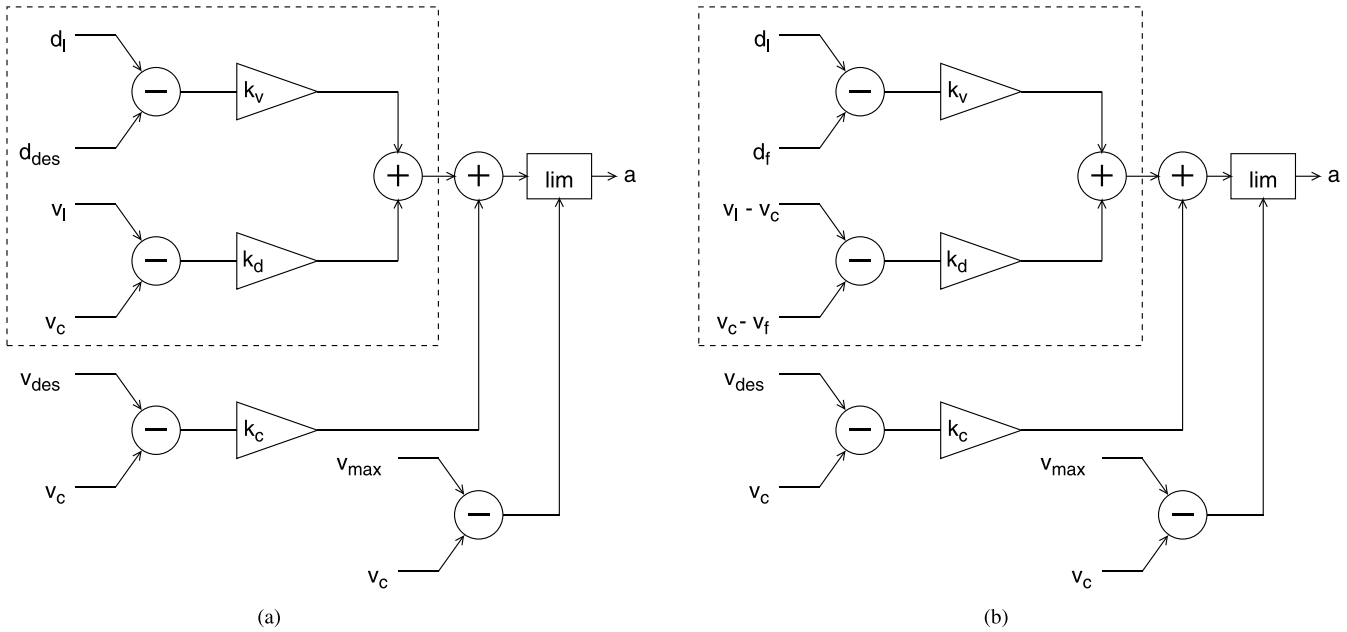

Fig. 3. (a) Illustrative car-following control system using distance and relative velocity of the leading car. The stability of a cascade of subsystems outlined in the dashed box is of interest here. (b)Illustrative bilateral control system using distance and relative velocity to leading *and* following car. The stability of a cascade of subsystems outlined in the dashed box is what is of interest.

Fig. 3(a) illustrates a simple car following control system which takes as input distance to (d_l), and relative speed of (v_l) the leading vehicle, and produces an acceleration command (a) at its output. In the figure, v_{des} is the speed desired by the driver, which may or may not be the same as the speed limit $v_{\max}$. Further, d_{des} is a desired separation, which may be a fixed quantity or may vary with speed as in "constant time headway" car following where $d_{\text{des}} = v_c T$, with T the "reaction time." The box labelled `lim` prevents positive acceleration when the current velocity v_c exceeds the speed limit $v_{\max}$ and enforces positive and negative limits on acceleration. (see Appendix A for details of the car following model). In contrast, Fig. 3(b) illustrates a bilateral control system which takes as inputs distances to (d_l and d_f), and relative speed of (($v_l - v_c$) and ($v_f - v_c$)) *both* following and leading vehicles. Again, additional inputs may include a desired speed v_{des}, and a speed limit $v_{\max}$.

Shown here is a simple model (which could be the result of linearizing a more complicated model about its current operating point). Here k_d is the gain for feedback based on the difference of the distances d_l and d_f to the leading and the following vehicles, while k_v is the gain for feedback based on the difference between the relative speeds ($v_l - v_c$) and ($v_c - v_f$). In addition, k_c is the (optional) gain of feedback based on the difference between the desired speed v_{des} and the current speed v_c (see also [1].) In both car following and bilateral control, amplification of perturbations along a chain of vehicles depends on the properties of the control subsystems in the dashed boxes.

For a practical implementation, additional components are needed to provide a complete model of vehicle control (see ch. 11 in [34], and [35]). This includes non-linear aspects and modes that deal with the case when (i) there is no leading vehicle, when (ii) there is no following vehicle, and (iii) emergency braking (needed in car following where traffic jams start to form).

When there is no following vehicle, a complete model can simply revert to traditional car following, and when there is no leading vehicle, control can devolve to traditional cruise control. Alternatively, if there is no following vehicle, a "virtual" following vehicle can be invoked that uses traditional car following, and the position and relative velocity of this virtual vehicle is used by the bilateral control system of the *actual* last vehicle in the chain of vehicles. Similarly, if there is no leading vehicle, a virtual vehicle can be invoked that uses simple cruise control and its position and relative velocity is used in bilateral control of the *actual* first vehicle in a chain of vehicles.

In the analysis of stability, we deal with a system linearized about the current operating point (corresponding to the dashed boxes in Fig. 3(a) and Fig. 3(b)). These linearized systems can capture the response to small perturbations of a number of different more "complete" models.

III. Vehicles Sequence Under Bilateral Control

First, in a simple linear model of car following, the acceleration of the controlled vehicle is given by

$$a = k_d(d_l - d_{\text{des}}) + k_v(v_l - v_c) \tag{1}$$

where k_d and k_v are the gains of positional and velocity feedback respectively ($k_d \geq 0$ and $k_v \geq 0$), and where d_{des} is a desired headway separation (which, in the case of "constant time headway" varies linearly with speed v_c).

In contrast, in a simple linear version of bilateral control, acceleration is given by [1],

$$a = k_d(d_l - d_f) + k_v\big((v_l - v_c) - (v_c - v_f)\big) \tag{2}$$

(Corresponding to $k_c = 0$ in Fig. 3(b)).

So, first, in the case of simple car following control, the acceleration of the n-th vehicle in the sequence is

$$\ddot{x}_n = k_d\big((x_{n+1} - x_n - l) - d_{\text{des}}\big) + k_v(\dot{x}_{n+1} - \dot{x}_n) \quad (3)$$

In contrast, in simple bilateral control, the acceleration of the n-th vehicle in the sequence can be written as

$$\ddot{x}_n = k_d(x_{n+1} - 2x_n + x_{n-1}) + k_v(\dot{x}_{n+1} - 2\dot{x}_n + \dot{x}_{n-1}) \quad (4)$$

where x_n, $\dot{x}_n$ and $\ddot{x}_n$ are the position, speed and acceleration of vehicle n.

The two expressions in parenthesis in eq. (4) can be thought of as finite differences that correspond to second order (spatial) derivatives of position x_n and of speed $\dot{x}_n$ respectively. We can replace this mixed continuous/discrete ordinary differential equation (ODE) in $x_n(t)$ with the continuous partial differential equation (PDE):

$$\frac{\partial^2 x}{\partial t^2} = k_d \frac{\partial^2 x}{\partial n^2} + k_v \frac{\partial^2}{\partial n^2}\frac{\partial x}{\partial t} \quad (5)$$

in $x(n, t)$. Note first that

$$x(n, t) = x_0 + dn + vt \quad (6)$$

is a solution, since this expression is linear in t and linear in n, so that second derivatives are all zero. This steady-state solution corresponds to vehicles uniformly spaced a distance d apart and travelling at common speed v.

IV. Separation of Variables

Other solutions of the PDE eq. (5) may be found using the method of separation of variables. Suppose that a particular solution $x(n, t)$ can be written as a product $N(n)T(t)$ of a function $N(n)$ of n and a function $T(t)$ of t, then

$$N(n)T''(t) = k_d N''(n)T(t) + k_v N''(n)T'(t) \quad (7)$$

or

$$\frac{N(n)}{N''(n)} = k_d \frac{T(t)}{T''(t)} + k_v \frac{T'(t)}{T''(t)} \quad (8)$$

This must be equal to a constant, since the left hand side of the equation is a function of n only and the right hand side is a function of t only. Without loss of generality, let this arbitrary constant be $-1/c^2$ (with $c \geq 0$). Then, from the left side of eq. (8), we have

$$N''(n) + c^2 N(n) = 0 \quad (9)$$

This second order ODE has solutions of the form

$$N(n) = A(c)e^{jcn} + A^*(c)e^{-jcn} \quad (10)$$

In practice, we are only interested in real solutions, which can be obtained by adding complex conjugate parts. We can obtain such solutions for different values of c (the spatial frequency of the wave). Linear combinations of such solutions, as well as the trivial solution eq. (6) are also solutions of the ODE eq. (9) since the differential equation is linear in the displacement. More complicated waveforms can thus be built up by adding sinusoidal waveforms of different spatial frequencies, with coefficients determined using transforms (Alternatively, one can just solve the PDE directly using Fourier or Laplace transform methods).

We also still have from the right side of eq. (8),

$$T''(t) + c^2 k_v T'(t) + c^2 k_d T(t) = 0 \quad (11)$$

Trying solutions of the form $T(t) = e^{st}$, we obtain the characteristic equation

$$s^2 + c^2 k_v s + c^2 k_d = 0 \quad (12)$$

with roots

$$s = -\frac{1}{2}c^2 k_v \pm \frac{1}{2}c\sqrt{c^2 k_v^2 - 4k_d} \quad (13)$$

Consider first the low frequency case when $c < 2\sqrt{k_d}/k_v$. Here s is complex and can be written $-\alpha \pm j\omega$, with

$$\alpha = \frac{1}{2}c^2 k_v \quad \text{and} \quad \omega = \frac{1}{2}c\sqrt{4k_d - c^2 k_v^2} \quad (14)$$

This corresponds to oscillatory solutions of (temporal) frequency ω, decaying with time constant $\tau = 1/\alpha$. In this case we have solutions for $x(n, t)$ of the form

$$x(n, t) = A_{\pm}(c)e^{-\alpha t}e^{j(\pm cn \pm \omega t)} \quad (15)$$

These are decaying waves travelling with speed $v = \pm(\omega/c)$.

In the high frequency case, on the other hand, when $c > 2\sqrt{k_d}/k_v$, we obtain two *real* roots for s—both of which are negative—corresponding to non-oscillatory exponentially decaying solutions.

V. Stabillity of Bilateral Control

For waves with low enough spatial frequency, where $c \ll 2\sqrt{k_d}/k_v$, we have $\omega \approx c\sqrt{k_d}$ and so $v \approx \pm\sqrt{k_d}$. Thus the speed of propagation of the decaying disturbances is proportional to the square root of the proportional gain. So the larger the proportional feedback gain k_d, the faster disturbances travel away from their source.

In the context of this paper, "stability" means that perturbations decay. This means that the amplitude of the response to complex exponential stimulation of any frequency must be smaller than the amplitude of the excitation. If we introduce a disturbance at some point in the system, the lower spatial frequency components will lead to waves travelling away from that point —in *both* directions—with speed $\sqrt{k_d}$. For $c > 0$, these waves decay with a time constant $\tau = 2/(c^2\ k_v)$. The steady-state solution, eq. (6) for $c = 0$, does not decay.

Higher spatial frequency components (shorter wavelengths) decay faster with distance than do lower frequencies. Note also that the rate of decay of travelling disturbances is proportional to the velocity gain constant k_v. So the larger the velocity feedback gain k_v, the faster disturbances die away.

Components of sufficiently high spatial frequency do not even lead to travelling waves and instead decay exponentially with two time constants, one smaller than $\tau = 1/\alpha$, and the other larger (reminiscent of evanescent waves in electromagnetic systems). We conclude that disturbances are dissipated, independent of spatial frequency content—only the steady-state solution, eq. (6), survives.

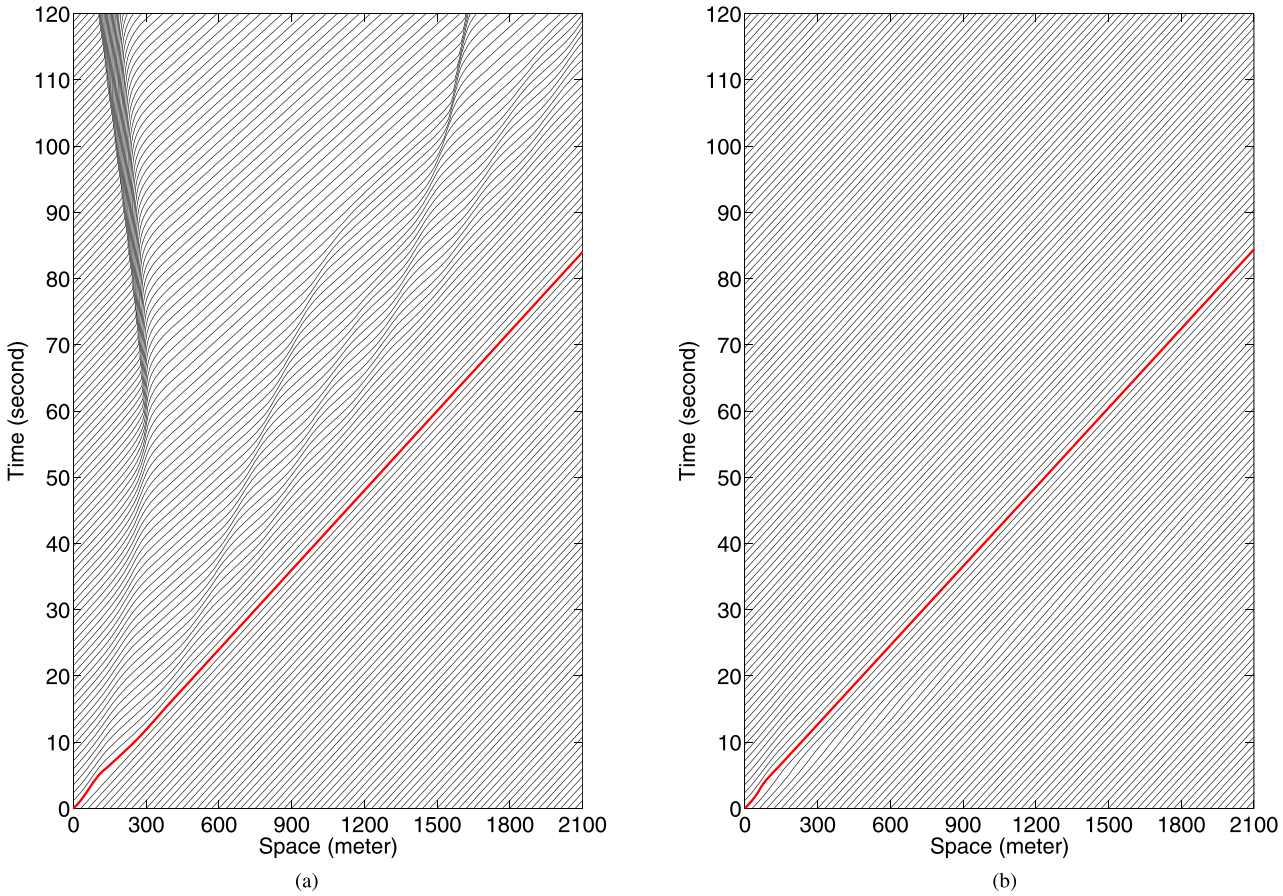

Fig. 4. (a) Car following control simulation (i.e. eq. (1), eq. (3)). The horizontal axis is distance in meters and the vertical axis is time in seconds. The progress of each vehicle is shown by a curve, which becomes vertical when the vehicle is stopped in traffic. A disturbance is injected by a vehicle starting at the lower left corner that brakes sharply after one second. Note traffic jam appearing at about 45 sec and moving upstream (i.e. to the left). (b) Bilateral control simulation in high density traffic (i.e. eq. (2), eq. (4)). Vehicle starting at lower left corner brakes sharply after one second, as in the previous figure. Damped waves of disturbances move downstream (right) and also upstream. No traffic jam develops and there is no long term disturbance of the flow.

It might appear that we could make the decay time constant $\tau = 1/\alpha$ arbitrarily small by making the speed gain k_v very large. Similarly, it would appear that we could make the decaying waves propagate away at arbitrarily high velocities by making the positional gain k_d very large. However, as is common in feedback systems, aspects of the real system not modeled in the simplified version will likely lead to instabilities when the gains become too large in the real system. (This includes effects due to unmodeled delays, and effects introduced by the approximation of the mixed continuous/discrete ODE by a continuous PDE.) Furthermore, passenger comfort would be impacted by high gain factors (leading to accelerations or decellerations higher than say ± 3 m/sec^2).

Note that in the sense of "stability" used here, simple car following is not stable, since it amplifies some frequency components (see [1], [36], [37] and Appendix A). An exception is a car following system with $k_d = 0$ and $k_v = 0$, which does not amplify disturbances at all, but, since it basically ignores traffic ahead, is of little practical interest.

VI. Independent Variable

It is important to note that the variable n in $x(n, t)$ is *not* the horizontal distance along the road, but is instead a continuous analog of the sequential vehicle number. That is, it increases by one as we move from one vehicle to the next. This means, first of all, that the wave velocities derived are relative to the moving traffic (not the road). Also, n increases more rapidly with distance along the road where vehicle density ρ is high than where density is low, since

$$\rho = \frac{dn}{dx} \tag{16}$$

So the speed of propagation of disturbances, when measured as track distance per unit time, is higher in areas of lower vehicle density (and slower in areas of higher density).

Importantly, the system does *not* obey a simple damped wave equation in the independent variable x, the distance along the road. This means, for example, that waves are *not* sinusoidal in the ground coordinate system.

This suggests an interesting non-linear modification of the basic linear bilateral control, where feedback contributions are weighted by vehicle density (i.e. inverse of vehicle spacing) so as to obtain constant speed of propagation of disturbances along the track (that is, constant in terms of distance along track per unit time rather than number of vehicles traversed per unit time). In this mode, adjustments to the vehicles speed are larger when the leading and following vehicle are nearby, and smaller when they are further away. Such a

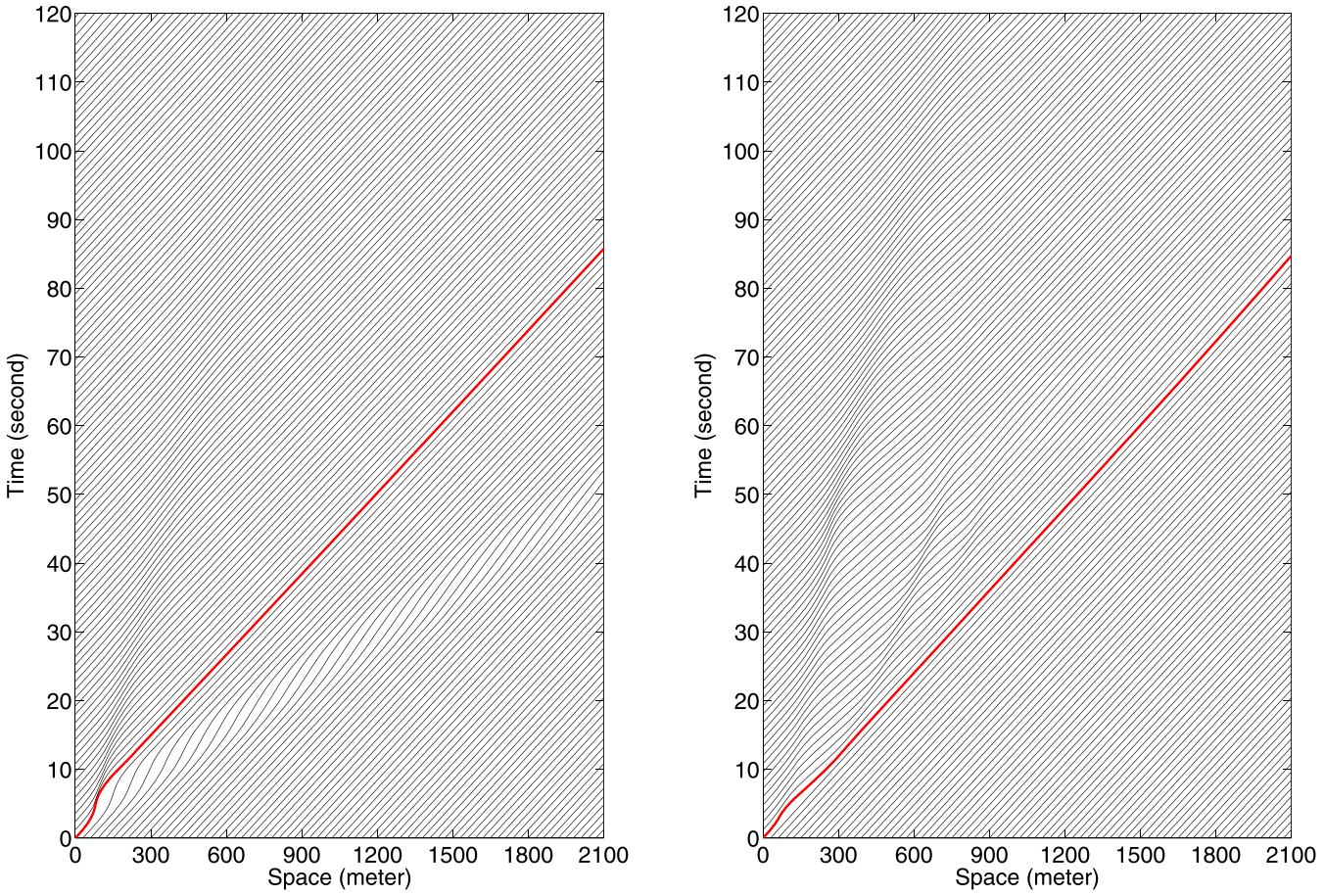

Fig. 5. (a) Bilateral control with four times as large a perturbation as in the previous figures. The downstream- and upstream-moving damped waves are more clearly visible. Still, no traffic jam results and there are no traffic flow instabilities. (b) Illustrating the ability of bilateral control to suppress impending traffic flow instabilities. Here, we start with car following control for 45 seconds, but then switch to bilateral control. The traffic jam developing under car following control is resolved under bilateral control, and the semi-periodic oscillations are suppressed as well.

system is governed by an ordinary damped wave equation with independent variable being the along track distance (x) rather than n.

VII. Simulation

We show here some results of simulations relating to traffic events that may lead to flow instabilities. Simulations, of course, merely illustrate the theoretical results, they cannot prove them. In the simulations below, the gains are

$$k_d = 0.4 \text{ sec}^{-2}$$
$$k_v = 0.2 \text{ sec}^{-1}$$
$$k_c = 0.02 \text{ sec}^{-1}$$

Other relevant parameters:

$$T = 1 \text{ sec}$$
$$l = 5 \text{ m}$$
$$v_{\text{des}} = 25 \text{ m/sec}$$
$$v_{\text{max}} = 30 \text{ m/sec}$$
$$a_{\text{min}},\ a_{\text{max}} = \pm 3 \text{ m/sec}^2$$

The car following simulations shown here implement the "constant time headway" method with $T = 1$ second (see Appendix A). For additional simulations, with different parameters, and a downloadable simulation application with controllable parameters, see online resource [38].

Fig. 4(a) shows a simulation of typical car-following behavior. The horizontal axis is distance in meters and the vertical axis is time in seconds. Each curve in Fig. 4(a) corresponds to one vehicle, with the slope of the curve being the inverse of its speed (becoming vertical when the vehicle is stopped in traffic). Vehicles exit the graphic on the right and new vehicles enter on the left. Initially all vehicles are moving at the same speed ($v = 25$ m/sec or 90 km/h)—corresponding to about a 45° angle in the graphic—with the same separation between them (30 m).

After a second, the vehicle that started at the origin (lower left) brakes hard—a deceleration of 5 m/sec^2—for two seconds (red trace). The resulting perturbation is propagated upstream—to the left of the vehicle. With car following, there is, of course, *no* effect on downstream vehicles (i.e. to the right of the vehicle that caused the disturbance).

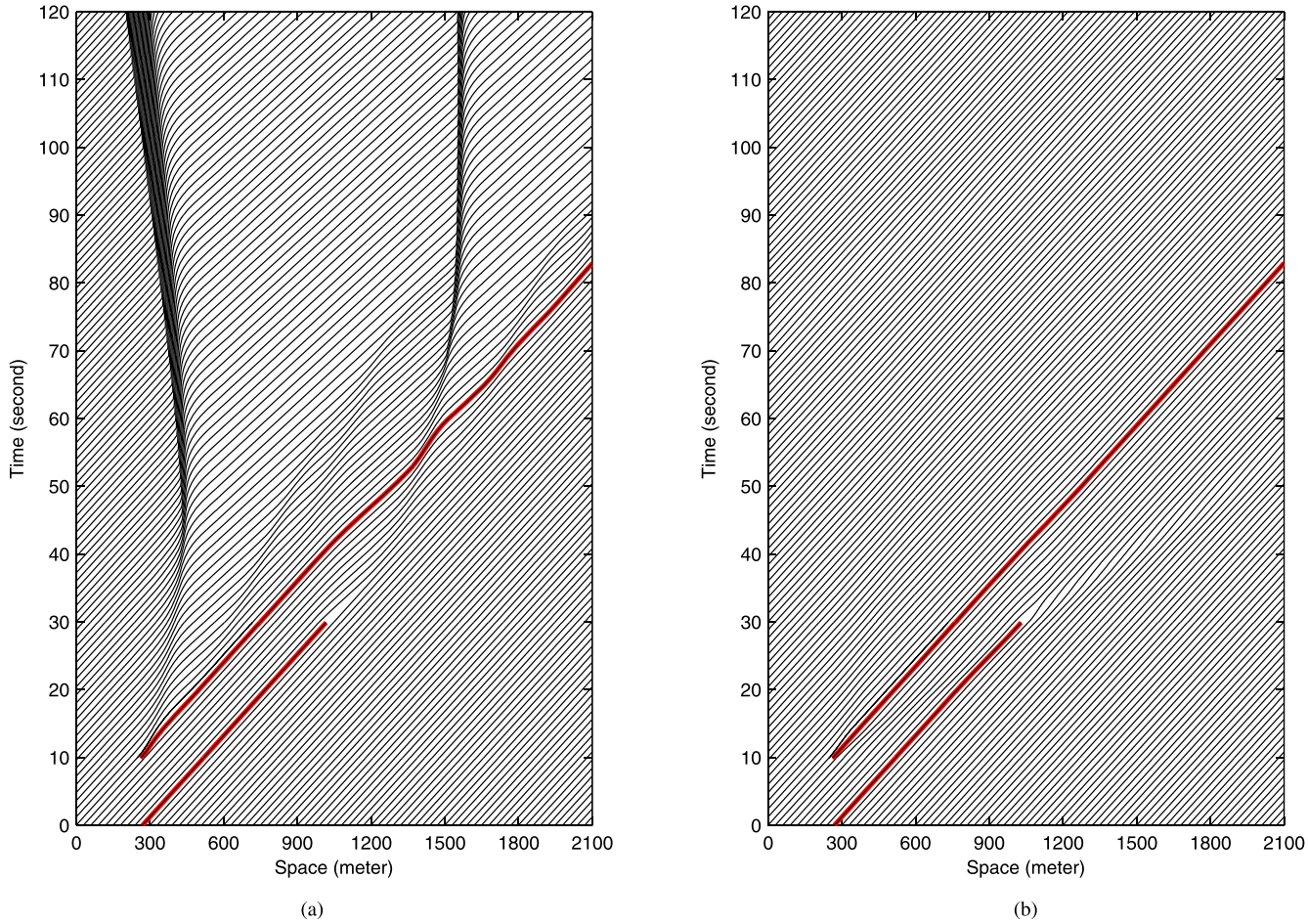

Fig. 6. Illustration of perturbations caused by lane changing in high traffic density. At 10 seconds, a car switches into the lane of traffic and at 30 seconds, a car moves out of the lane. (a) In car-following control, perturbations are amplified as they propagate away from their source. (b) Bilateral control suppresses potential perturbations resulting from lane changing. Perturbations are attenuated as they propagate away from their source.

The perturbation is amplified as it is propagated backward and leads to a pile-up starting around 45 seconds. The upstream edge of the traffic jam moves backward (left leaning slope) at about 3.8 m/sec (13.5 km/h), which is the arrival rate of roughly 0.83 vehicles per second times the average vehicle length of 5 m. This corresponds to observed behavior of actual "stop-and-go" traffic flow instabilities and so-called "phantom traffic jams" (see Fig. 2 in [39]).

There are, by the way, also some smaller, semi-periodic fluctuations to the right of the jam, and additional structure appears above if the plot is continued for longer times (upwards). Interestingly, after the initial disturbance, there are no effects near the vehicle that was the distal cause of the problem. Note that because of the amplification of perturbations in the car following model, even smaller variations in speed can lead to instabilities [1].

In stark contrast, Fig. 4(b) shows a simulation under bilateral control, with the same control system gains and the same disturbance. With bilateral control, the disturbance has the effect of generating damped waves moving both forward and backward in traffic. In this particular case, the forward moving wave is of a dilationary nature, while the backward moving wave is compressive.

The travelling wave effects are small and not so easily discerned for this size of disturbance. To make the damped waves appear more clearly, Fig. 5(a) shows a simulation with a perturbation that is four times as large (in terms of change of speed). The two damped waves spreading from the disturbed vehicle are more easily seen. The speed of the damped waves (relative to the traffic flow) here is $v = \pm\sqrt{k_d} = \pm\sqrt{0.4} = \pm 0.632\ldots$. This is, of course, a speed expressed in terms of vehicles per second, but can be converted to meters per second if the local density of vehicles is known. For a density of $1/30$ vehicles per meter (33 vehicles per km), this comes to about 19 m/sec. So the forward moving wave moves at approximately 44 m/sec (i.e. $25 + 19$) and the backward moving wave moves at approximately 6 m/sec (i.e. $25 - 19$), as can be seen in Fig. 5(a).

To illustrate the ability of bilateral control to suppress impending instabilities, Fig. 5(b) shows a simulation where we start with the system under car following control but then switch to bilateral control at 45 seconds. The traffic jam just starting to form at that point in time soon dissipates (as do the semi-periodic fluctuations further downstream).

The system is also immune to disturbances resulting from lane changing, merging and splitting of lanes. Fig. 6(a) shows

a simulation of car following where a car leaves the lane of traffic and another car switches into the lane of traffic. Fig. 6(b) shows a simulation of bilateral control under the same circumstances. The disturbances die away smoothly.

VIII. Conclusion

Sequences of vehicles under bilateral control can be modelled by a second order PDE—but where the independent variable is *not* the distance along the road. The solutions of the PDE are damped waves travelling in both directions from a disturbance. The effects of perturbations are attenuated rather than amplified. Simulations illustrate the analytical results. Importantly, sequences of vehicles under car following control do *not* satisfy such an equation because information flow is unidirectional (up-stream only).

It should be noted that car following models with "constant time headway" instead of "constant space headway" (as in eq. 1) *can* be made string stable by using sufficiently high control gains. But, as discussed in Appendix A, higher gains k_d and k_v come with changes that may reduce throughput and may impact passenger comfort. There are no corresponding restrictions on these gains in bilateral control systems (just that they be positive).

Implementing bilateral control will be well worth the effort since it will reduce travel times, fuel consumption and greenhouse gas emissions. Existing infrastructure need not be modified—yet higher traffic throughput can be supported. This is a good time to start implementing bilateral control, since vehicles with adaptive cruise control already have the required control mechanisms, as well as the forward facing sensors. All that is required is addition of rearward facing sensors and a change in the control algorithm to bilateral control as presented here.

Appendix A
Car Following Control Perturbation Gain

There is a vast literature—going back 80 years now—describing traffic flow instabilities and explaining their origin in various ways [7]–[25]. The focus in this paper, in contrast, has been on a method for *preventing* such instabilities (and suppressing them should they occur as the result of unexpected external inputs).

It may nevertheless be worth briefly looking at the car following problem yet again. We show here that in the car following control model, there are always frequencies of disturbances that are amplified as they are propagated upstream from their source (The disturbance could, for example, be due to a difference in speed when one vehicle applies the brakes briefly.) The gain per stage (vehicle) can be determined by analyzing a simple model. In car following control we have

$$\ddot{x}_c = k_d\big((x_l - x_c - l) - d_{\text{des}}\big) + k_v(\dot{x}_l - \dot{x}_c) \tag{17}$$

where $\ddot{x}_c$ is the acceleration of the controlled vehicle, $\dot{x}_c$ and $\dot{x}_l$ are the speeds of the controlled vehicle and the leading vehicle, x_c and x_l are the positions of the controlled vehicle and the leading vehicle [1]. The desired (safe) separation between vehicles is d_{des}, and the gain constants are k_d for positional control and k_v for velocity control. Then

$$\ddot{x}_c + k_v\dot{x}_c + k_d x_c = k_v\dot{x}_l + k_d(x_l - l - d_{\text{des}}) \tag{18}$$

This linear relationship corresponds to a simple version of the "Helly model" for car following control [26], [40], [41].

This is clearly a linear shift invariant system, and it is well known that exponential functions of time are eigenfunctions of such systems. Suppose then that $x_l = e^{st} + l + d_{\text{des}}$ then $x_c = Ae^{st}$ where

$$A = \frac{k_v s + k_d}{s^2 + k_v s + k_d} \tag{19}$$

For sinusoidal excitation, $s = j\omega$ and

$$A = \frac{k_d + j\omega k_v}{(k_d - \omega^2) + j\omega k_v} \tag{20}$$

$$|A|^2 = A^*A = \frac{k_d^2 + (\omega k_v)^2}{(k_d - \omega^2)^2 + (\omega k_v)^2} \tag{21}$$

We see that $A = 1$ for $\omega = 0$ and $|A| = 1$ for

$$\omega_1 = \sqrt{2k_d}. \tag{22}$$

since $(k_d - \omega_1^2) = -k_d$. Importantly, the magnitude of the gain, $|A|$, of one stage of the system (i.e. one vehicle) is greater than 1 for $0 < \omega < \omega_1$. The magnitude of the gain reaches a peak at

$$\omega_{\max} = \frac{k_d}{k_v}\sqrt{\sqrt{1 + 2k_v^2/k_d} - 1} \tag{23}$$

The important things is that the gain is greater than 1 for a range of low frequencies and so corresponding components of the perturbations will be amplified along the chain. So simple car following systems are unstable, since the gain is greater than 1 for $0 < \omega < \omega_1$, no matter what the control gain parameters k_d and k_v are (as long as $k_d > 0$).

The simple car following model assumes that the desired separation d_{des} between vehicles is constant. For safety it is best that the desired separation vary with speed. The "constant time headway" distance is $d_{\text{des}} = vT$, where v is the speed of the vehicles and T the "reaction time" (see Appendix B). This improvement on the simple "constant headway" car following model is called the "constant time headway" model. (see also [42], [43]). We can analyze this much the same way as the simple car following model. We have

$$\ddot{x}_c + (k_v + k_d T)\dot{x}_c + k_d x_l = k_v\dot{x}_l + k_d(x_l - l) \tag{24}$$

So

$$A = \frac{k_v s + k_d}{s^2 + (k_v + k_d T)s + k_d} \tag{25}$$

For sinusoidal excitation, $s = j\omega$ and

$$A = \frac{k_d + j\omega k_v}{(k_d - \omega^2) + j\omega(k_v + k_d T)} \tag{26}$$

$$|A|^2 = A^*A = \frac{k_d^2 + (\omega k_v)^2}{(k_d - \omega^2)^2 + \omega^2(k_v + k_d T)^2} \tag{27}$$

In this case, $|A| < 1$ if

$$2k_v T + k_d T^2 - 2 > 0 \tag{28}$$

or

$$k_v + k_d T/2 > 1/T \tag{29}$$

as shown in [40]. It should be noted, however, that typically T is taken to be about 1 second (Appendix B), so rather large gains (k_v and k_d) are implied. Alternatively, for given feedback gains k_v and k_d we can try and satisfy the condition by making T large. Then we require

$$T > \frac{-k_v + \sqrt{k_v^2 + 2k_d}}{k_d} \tag{30}$$

For $k_d = 0.4$ sec^{-2} and $k_v = 0.2$ sec^{-1}, for example (as used in the simlations here), this yields $T = 1.79\ldots$ seconds, which implies inter-vehicle gaps almost twice as large as is common, and thus a considerable reduction in throughput. In this regard, note that the flow (vehicles per second) is given by

$$\rho v = \frac{v}{l + vT} \tag{31}$$

where ρ is the density and l vehicle length. The flow approaches $1/T$ asymptotically as speed increases. So making T large means lowering the throughput.

Appendix B
Improved Safe Following Distance Formula

It is easy to show that

$$d_1 = vT \tag{32}$$

is the safe following distance, where v is the speed of the vehicles and T the reaction time. Reaction time here is meant to include not just perceptual and mental processes, but shifting the foot from accelerator to brake and delay in the response of the vehicle. Reaction time is typically taken to be about 1 second (or a little more). Assuming a typical vehicle length of 4.6 m (15') this leads to the familiar formula for safe distance: "about one vehicle length per 16 km/h (10 mph)."

The derivation of formula eq. (32) assumes that the vehicles can decelerate at the same rate, and that they are initially travelling at the same speed. In practice this is rarely the case, particularly when drivers (or vehicle control systems) are busy adjusting speeds in order to come closer to travelling with the 'minimum safe separation' between them. Not surprisingly, the gap needs to be larger if the following vehicle is moving faster than the leading vehicle, and, correspondingly, can be smaller if the following vehicle is moving more slowly, as shown next.

Suppose the leading vehicle is travelling at speed v_{10} at time t_1 when its brakes are engaged. Then

$$v_1(t) = v_{10} + a_1(t - t_1) \tag{33}$$

where the a_1 is the acceleration when braking ($a_1 < 0$). The speed will be zero at time t_{1z} where

$$t_{1z} = t_1 + \frac{v_{10}}{(-a_1)} \tag{34}$$

The position of the leading vehicle on the road will be

$$x_1(t) = x_{10} + v_{10}(t - t_1) + \frac{1}{2}a_1(t - t_1)^2 \tag{35}$$

which comes to

$$x_{1z} = x_{10} + \frac{1}{2}\frac{v_{10}^2}{(-a_1)} \tag{36}$$

when the leading vehicle comes to a stop at $t = t_{1z}$. Similarly, suppose the following vehicle is travelling at speed v_{20} at time t_2 when *its* brakes are engaged. Then the position of that vehicle will be

$$x_{2z} = x_{20} + \frac{1}{2}\frac{v_{20}^2}{(-a_2)} \tag{37}$$

when it comes to a stop at time t_{2z}. We have $x_{2z} = x_{1z}$ if

$$d_2 = x_{10} - x_{20} = \frac{1}{2}\frac{v_{20}^2}{(-a_2)} - \frac{1}{2}\frac{v_{10}^2}{(-a_1)} \tag{38}$$

This is the minimum initial separation needed to avoid a collision. If the braking capabilities of the two vehicles are the same then

$$d_2 = \frac{v_{20}^2 - v_{10}^2}{-2a} \tag{39}$$

or

$$d_2 = \frac{(v_{20} + v_{10})}{2}\frac{(v_{20} - v_{10})}{(-a)} \tag{40}$$

so d_2 is proportional to the product of the average speed of the two vehicles and the difference in their speeds (divided by the braking deceleration).

We have not yet taken into account the reaction time. In practice we need to add the value $d_1 = v_{20}T$ to the separation d_2 derived above to allow for the reaction time.

So the gap has to be larger than the 'minimum safe separation' $d_1 = v_{20}T$ when $v_{20} > v_{10}$, and can be smaller when $v_{20} < v_{10}$ (see also [42]). The improved 'minimum safe distance,' $d_{\min} = d_1 + d_2$, is not likely to be of direct use to a human driver, because it requires some calculation and knowledge of the speeds of both vehicles. But such a calculation can be easily incorporated in an automated feedback system. Simulation shows that use of this modified 'safe distance' algorithm helps reduce—but does not eliminate—traffic flow instabilities (unless bilateral control is implemented).

References

[1] B. K. P. Horn, "Suppressing traffic flow instabilities," in *Proc. IEEE Intell. Transp. Syst.*, The Hague, The Netherlands, Oct. 2013, pp. 13–20.

[2] D. Schrank, N. Eisele, and T. Lomax, "TTI's 2012 urban mobility report," Texas A&M Transp. Inst., College Station, TX, USA, Dec. 2012. [Online]. Available: http://mobility.tamu.edu

[3] A. A. M. Aljanahi, A. H. Rhodes, and A. V. Metcalfe, "Speed, speed limits and road traffic accidents under free flow conditions," *Accident Anal. Prevention*, vol. 31, pp. 161–168, Jan. 1999.

[4] E. M. Ossiander and P. Cummings, "Freeway speed limits and traffic fatalities in washington state," *Accident Anal. Prevention*, vol. 34, no. 1, pp. 13–18, 2002.

[5] T. A. Baran and B. K. P. Horn, "A robust signal-flow architecture for cooperative vehicle density control," in *Proc. IEEE Int. Conf. Acoust., Speech Signal Process. (ICASSP)*. Vancouver, BC, Canada, May 2013, pp. 2790–2794.

[6] L. Wang, B. K. P. Horn, and G. Strang, "Eigenvalue and eigenvector analysis of stability for a line of traffic," *Stud. Appl. Math.*, vol. 138, no. 1, pp. 103–132, Jan. 2017.

[7] B. D. Greenshields, J. R. Bibbins, W. S. Channing, and H. H. Miller, "A study of traffic capacity," *Proc. Highway Res. Board*, vol. 14, pp. 448–477, 1935.

[8] M. J. Lighthill and G. B. Whitham, "On kinematic waves. II. A theory of traffic flow on long crowded roads," *Proc. Roy. Soc. London A, Math. Phys. Sci.*, vol. 229, no. 1178, pp. 317–345, May 1955.

[9] G. F. Newell, "Mathematical models for freely-flowing highway traffic," *J. Oper. Res. Soc. Amer.*, vol. 3, no. 2, pp. 176–186, May 1955.

[10] P. I. Richards, "Shock waves on the highway," *Oper. Res.*, vol. 4, no. 1, pp. 42–51, 1956.

[11] R. E. Chandler, R. Herman, and E. W. Montroll, "Traffic dynamics: Studies in car following," *Oper. Res.*, vol. 6, no. 2, pp. 165–184, 1958.

[12] R. Herman, E. W. Montroll, R. B. Potts, and R. W. Rothery, "Traffic dynamics: Analysis of stability in car following," *Oper. Res.*, vol. 7, no. 1, pp. 86–106, 1959.

[13] L. C. Edie, "Car-following and steady-state theory for noncongested traffic," *Oper. Res.*, vol. 9, no. 1, pp. 66–76, 1961.

[14] J. Treiterer and J. A. Myers, "The hysteresis phenomena in traffic flow," in *Proc. 6th Symp. Transp. Traffic Theory*, 1974, pp. 13–38.

[15] B. S. Kerner and H. Rehborn, "Experimental properties of phase transitions in traffic flow," *Phys. Rev. Lett.*, vol. 79, pp. 4030–4033, Nov. 1997.

[16] D. Helbing and B. A. Huberman, "Coherent moving states in highway traffic," *Nature*, vol. 396, pp. 738–740, Sep. 1998.

[17] H. Y. Lee, H.-W. Lee, and D. Kim, "Origin of synchronized traffic flow on highways and its dynamic phase transitions," *Phys. Rev. Lett.*, vol. 81, pp. 1130–1133, Aug. 1998.

[18] C. F. Daganzo, M. J. Cassidy, and R. L. Bertini, "Possible explanations of phase transitions in highway traffic," *Transp. Res. A, Policy Pract.*, vol. 33, no. 5, pp. 365–379, 1999.

[19] T. Nagatani, "Traffic jams induced by fluctuation of a leading car," *Phys. Rev. E, Stat. Phys. Plasmas Fluids Relat. Interdiscip. Top.*, vol. 61, pp. 3534–3540, Apr. 2000.

[20] E. Tomer, L. Safonov, and S. Havlin, "Presence of many stable nonhomogeneous states in an inertial car-following model," *Phys. Rev. Lett.*, vol. 84, pp. 382–385, Jan. 2000.

[21] L. C. Davis, "Effect of adaptive cruise control systems on traffic flow," *Phys. Rev. E, Stat. Phys. Plasmas Fluids Relat. Interdiscip. Top.*, vol. 69, p. 066110, Jun. 2004.

[22] B. S. Kerner, *The Physics of Traffic*. New York, NY, USA: Springer, 2004.

[23] G. Orosz and G. Stépán, "Subcritical Hopf bifurcations in a car-following model with reaction-time delay," *Proc. Roy. Soc. A, Math., Phys. Eng. Sci.*, vol. 462, no. 2073, pp. 2643–2670, 2006.

[24] B. S. Kerner, *Introduction to Modern Traffic Flow Theory and Control*. New York, NY, USA: Springer, 2009.

[25] J. A. Laval and L. Leclercq, "A mechanism to describe the formation and propagation of stop-and-go waves in congested freeway traffic," *Philos. Trans. Roy. Soc. A, Math., Phys. Eng. Sci.*, vol. 368, no. 1928, pp. 4519–4541, 2010.

[26] M. Brackstone and M. McDonald, "Car-following: A historical review," *Transp. Res. F, Traffic Psychol. Behavior*, vol. 2, no. 4, pp. 181–196, 1999.

[27] D. Chowdhury, L. Santen, and A. Schadschneider, "Statistical physics of vehicular traffic and some related systems," *Phys. Rep.*, vol. 329, nos. 4–6, pp. 199–329, 2000.

[28] D. Helbing, "Traffic and related self-driven many-particle systems," *Rev. Mod. Phys.*, vol. 73, no. 4, p. 1067, 2001.

[29] T. Nagatani, "The physics of traffic jams," *Rep. Progr. Phys.*, vol. 65, no. 9, p. 1331, 2002.

[30] A. Schadschneider, D. Chowdhury, and K. Nishinari, *Stochastic Transport in Complex Systems: From Molecules to Vehicles*. Amsterdam, The Netherlands: Elsevier, 2010.

[31] A. Nakayama, Y. Sugiyama, and K. Hasebe, "Effect of looking at the car that follows in an optimal velocity model of traffic flow," *Phys. Rev. E, Stat. Phys. Plasmas Fluids Relat. Interdiscip. Top.*, vol. 65, no. 1, p. 016112, 2001.

[32] L. Zheng, P. J. Jin, and H. Huang, "An anisotropic continuum model considering bi-directional information impact," *Transp. Res. B, Methodol.*, vol. 75, pp. 36–57, May 2015.

[33] M. Treiber and D. Helbing, "Hamilton-like statistics in onedimensional driven dissipative many-particle systems," *Eur. Phys. J. B*, vol. 68, no. 4, pp. 607–618, 2009.

[34] M. Treiber and A. Kesting, *Traffic Flow Dynamics: Data, Models and Simulation*. Berlin, Germany: Springer Verlag, 2013.

[35] P. A. Ioannou, Ed., *Automated Highway Systems*. New York, NY, USA: Plenum, 1997.

[36] S. E. Shladover, "Longitudinal control of automated guideway transit vehicles within platoons," *ASME J. Dyn. Syst., Meas., Control*, vol. 100, no. 4, pp. 302–310, 1978.

[37] S. Sheikholeslam and C. A. Desoer, "Longitudinal control of a platoon of vehicles," in *Proc. Amer. Control Conf.*, San Diego, CA, USA, May 1990, pp. 291–296.

[38] B. K. Horn. *Traffic Flow Instabilities*. Accessed: Nov. 1, 2015. [Online]. Available: http://people.csail.mit.edu/bkph/Traffic_Flow_Animation

[39] B. S. Kerner and P. Konhäuser, "Structure and parameters of clusters in traffic flow," *Phys. Rev. E, Stat. Phys. Plasmas Fluids Relat. Interdiscip. Top.*, vol. 50, no. 1, p. 54, 1994.

[40] C.-Y. Liang and H. Peng, "Optimal adaptive cruise control with guaranteed string stability," *Veh. Syst. Dyn., Int. J. Veh. Mech. Mobility*, vol. 32, nos. 4–5, pp. 313–330, 1999.

[41] M. Wang, W. Daamen, S. P. Hoogendoorn, and B. van Arem, "Rolling horizon control framework for driver assistance systems. Part II: Cooperative sensing and cooperative control," *Transp. Res. C, Emerg. Technol.*, vol. 40, pp. 290–311, Mar. 2014.

[42] P. A. Ioannou and C. C. Chien, "Autonomous intelligent cruise control," *IEEE Trans. Veh. Technol.*, vol. 42, no. 4, pp. 657–672, Nov. 1993.

[43] P. Ioannou and Z. Xu, "Throttle and brake control systems for automatic vehicle following," *IVHS J.*, vol. 1, no. 4, pp. 345–377, 1994.

Berthold K. P. Horn received the B.Sc. Eng. degree from the University of the Witwatersrand in 1965 and the S.M. and Ph.D. degrees from Massachusetts Institute of Technology (MIT) in 1968 and 1970, respectively. He is currently a Professor of electrical engineering and computer science with MIT. He is the author, co-author, or editor of books on the programming language LISP and machine vision, including robot vision.

Dr. Horn received the Rank Prize for pioneering work leading to practical vision systems in 1989 and was elected a Fellow of the American Association of Artificial Intelligence in 1990 for significant contributions to artificial intelligence. He was elected to the National Academy of Engineering in 2002 and received the Azriel Rosenfeld Lifetime Achievement Award from the IEEE Computer Society for pioneering in early vision in 2009. His current research interests include machine vision, computational imaging, and intelligent vehicles.

Liang Wang was born in 1983. He received the B.S. and M.S. degrees in electronic engineering from the School of Electronic and Information Engineering, Beijing Jiaotong University, in 2006 and 2008, respectively, and the Ph.D. degree in computer application technology from the School of Computer and Information Technology, Beijing Jiaotong University.

He studied in the Mathematics Department, Massachusetts Institute of Technology (MIT), from 2011 to 2013, supervised by Prof. G. Strang. He is currently a Post-Doctoral Research Scholar with CSAIL, Department of Engineering and Computer Science, MIT. His research interests include machine vision and inverse problems.